Experimental report

09/08/2018

Proposal: **TEST-2894** **Council:** 4/2018

Title: Slective Disruption Mechanisms of Surfactant-Like Antimicrobial Peptides with the Outer and Inner Membranes of Gram-Negative Bacteria

Research area:

This proposal is a new proposal

Main proposer: **Haoning GONG**

Experimental team: Ke FA
Haoning GONG

Local contacts: Armando MAESTRO

Samples: DPPG
RcLPS
Peptide (G3)

Instrument	Requested days	Allocated days	From	To
FIGARO	2	2	06/06/2018	08/06/2018

Abstract:

Lipopolysaccharide Functions as the Bacterial Receptors to the Antimicrobial Peptides

Haoning Gong[1], Ke Fa[1], Armando Maestro[2], Jian R Lu[1]
[1]University of Manchester, Manchester M13 9PL UK
[2]Institut Laue-Langevin, 71 avenue des Martyrs, CS20156, 38042 Grenoble, Cedex 9, France

Proposal: Test-2894
Dates: 7-8.06.2018

Introduction

Antimicrobial peptides (AMPs) kill pathogenic microbes via a membrane disruptive mechanism. Because it is a fast physical action, microbes are unable to quickly evolve a counter-responsive mechanism to develop antimicrobial resistance (AMR). We have developed a series of novel surfactant-like cationic α-helical AMPs using the general formula $G(IIKK)_nI\text{-}NH_2$ (n=1-4, denoted as G_1 – G_4) [1]. Among them, G_3 has displayed potent antimicrobial activity matched with good biocompatibility. Reconstructed lipid monolayers (DPPG, DPPC, POPG) at the air/water interface and their interactions with G_4 have been studied by neutron reflection (NR) on FIGARO to investigate how AMPs bind and disrupt the model membrane leaflets via selectivity towards anionicity or saturation of the phospholipids [2-3]. Additionally, NR studies of the interactions of G_4 with lipopolysaccharide (LPS) monolayers have been employed to investigate how the bacterial outer membrane acts as the protection layer to prevent any AMP invasion. A manuscript has been drafted to describe the above work for publication. In addition to the G_4 work against different lipid models, novel AMPs have been developed to improve their potency whilst tuning biocompatibility. Recent studies have revealed that some AMPs are strain-specific. The LPS leaflet of the Gram-negative bacteria could act as the receptor to some AMPs. In this experiment we have examined how $C_8\text{-}G_2$ (P2), G_3, $KKK(KKII)_2II\text{-}NH_2$ (P11) interact with either LPS or DPPG monolayers, mimicking either the outer leaflet or inner leaflet of the Gram-negative bacteria. The NR data have helped unravel different structural features underlying membrane disruptions leading to the selective killing of bacteria.

Materials and Methods

We constructed the DPPG and RcLPS monolayers at the air/water interface using a Langmuir trough (Nima Technology Ltd, Coventry, UK). The air/water interface was created upon 80 ml PBS buffer (pH=7.4). DPPG and RcLPS were dissolved in chloroform/methanol (9:1, v/v) and chloroform/methanol/water (65:30:5, v/v/v), and titrated onto the air/water interface to construct the lipid monolayers. Surface pressures of all the lipid monolayers were initially controlled to be 28 mN/m. 4 isotropic contrasts were carried out by producing either deuterated or protonated lipid monolayers onto the null reflecting water (NRW) or D_2O, respectively. Concentrated peptide solutions were injected underneath the lipid monolayers to produce the required peptide concentrations (3 and 30 μM). The NR experiments were carried out at angles of 0.62° and 3.8°, respectively.

In NR data analysis, the kinetic procedures of lipid loss and peptide adsorption upon peptide binding were derived by the low Q-range data treatment of both deuterated and hydrogenated lipids with and without peptides in NRW. The structural characteristics of the lipid monolayers with and without peptides were resolved by the full Q-range data analysis involving all 4 isotropic contrasts.

Results

To mimic the physiological conditions of real membranes, the lipid monolayers were compressed to the initial pressure of 28 mN/m under which the monolayer structures were determined by NR. Figure 1 shows the reflectivity profiles measured from the RcLPS monolayers under 4 isotropic contrasts with and without peptide bindings. The main structural parameters as resolved from the 4 contrast fits were presented in Table 1. The area per molecule obtained from the RcLPS and DPPG monolayers at 28 mN/m was 198 ± 2 Å, 48 ± 2 Å^2, respectively. An RcLPS and a DPPG molecule has 6 and 2 acyl chains in the hydrophobic tail regions, respectively. Thus, the area per chain of the RcLPS and DPPG monolayers were calculated to be 33 Å, 24 Å^2, which revealed that the DPPG monolayers were more compressed than the RcLPS monolayers at 28 mN/m. This is well expected because the RcLPS molecules carry unsaturated acyl chains, which have bent structures rather than straight tails as in DPPG molecules. The tail groups of the RcLPS layer was characterised to be 13 ± 1 Å thick, smaller than that of DPPG with the thickness of 18 ± 2 Å. In contrast, the head groups of the RcLPS were determined to be 23 ± 2 Å thick, significantly larger than the DPPG monolayers with the thickness of 10 ± 1 Å. The larger head group thickness in RcLPS implies greater compression, consistent with the easier penetration of the peptide into the head group region of the DPPG monolayer.

After injection of G_3 at 3 μM, 8% LPS molecules were found to be lost into the buffer subphase with G_3 adsorption of 0.04 μmol/m^2 and 0.08 μmol/m^2 to the tail and head regions, respectively. With the increase of G_3 concentration up to 30 μM, 38% LPS molecules were removed, indicating substantial destruction to the lipid layer structure. Additionally, 0.33 μmol/m^2 of G_3 were found to bind with either the tail or head groups, with the

addition of 0.26 μmol/m^2 G_3 further adsorbed beneath the head layer in the buffer subphase. In contrast, only 15% DPPG molecules were lost upon exposure to either 3 μM or 30 μM G_3. As discussed above, DPPG monolayers were more compressed in the tail region than the LPS monolayers, thus were more stable upon peptide binding and dissolution. Because of the relatively longer tail of DPPG (18 Å), even if the lipid layer is porous with water penetrated to the tail region after the structural disruption, DPPG molecules tended to stay at the air/water interface rather than dissolved to the buffer subphase like LPS. Upon increasing G_3 concentrations from 3 μM to 30 μM against DPPG monolayers, water penetration to the tail regions were increased from 10% to 15% of volume fraction with the G_3 binding from 0.17 μmol/m^2 to 0.31 μmol/m^2, respectively. Thus, the increased water penetration and peptide binding to the lipid tail region were the key indicators of the structural disruption to the lipid monolayers.

P_2 peptide was derived from G_2 peptide by incorporating a C_8 fatty acid chain to its N-terminal, which significantly improved peptide's hydrophobicity. Because of the strong hydrophobicity, P_2 removed most LPS (47% and 55% loss at 3 μM to 30 μM AMP concentrations) among the AMPs tested. There were 0.61 μmol/m^2 and 0.7 μmol/m^2 P_2 binding to the LPS tail regions at two tested AMP concentrations, significantly higher than G_3 at the corresponding concentrations. Only 0.1 μmol/m^2 P_2 were found at the LPS head regions in either low or high AMP concentrations. But there was an additional peptide layer adsorbed beneath the head regions with the amount of 0.18 μmol/m^2. In contrast, there were 8% DPPG loss after interactions with 3 μM to 30 μM of P_2 peptides. Similar to the LPS model, 0.32 μmol/m^2 and 0.43 μmol/m^2 of P_2 reached the tail regions, whilst there were 0.04 μmol/m^2 and 0.72 μmol/m^2 P_2 went to the head groups at the peptide concentrations, respectively. It should be noticed that a remarkable amount of P_2 peptide at 30 μM penetrated into the DPPG tail group region with the amount of 0.36 μmol/m^2, consistent with its strong membrane disruption. In comparison with G_3, P_2 peptide was more disruptive to either the LPS or DPPG monolayers. But its strong attraction to lipids may hinder its antimicrobial efficacy.

P_{11} peptide was the cationic derivative of the G_3 peptide by introducing excess positively charged amino acid Lysine (K) to make it more cationic but far less hydrophobic. Because of the weak hydrophobic nature, P_{11} peptide was found to be the weakest one amongst the tested peptides. There was only 5% DPPG loss after interaction with P_{11} peptide at high concentration (30 μM). Only 0.07 μmol/m^2 of P_{11} was found to penetrate to the tail region of DPPG, but 0.53 μmol/m^2 was bound to the head region, showing the strong electrostatic interaction with the anionic phosphate groups. Microbial membranes carry partial negatively charged phospholipids (e.g. PG and CL) by incorporating neutral components (e.g. PE and PC). Thus P_{11} should have weak ability to kill any bacteria. However, P_{11} had a 4 μM MIC against *E. coli*, even lower than G_3 and P_2 peptides. Thus, its interaction with the LPS monolayers can be used to reveal why P_{11} can selectively kill *E. coli*. It was found that at 3 μM, 0.1 μmol/m^2 of P_{11} went to the LPS tail regions and 0.44 μmol/m^2 adsorbed to the head groups. Compared with G_3 peptides at 3 μM, P_{11} had similar extent of interaction to the LPS layer. However, with the increase of peptide concentrations, more P_{11} originally attached to the head regions can penetrate to the tail regions without any further adsorption. Because of the strong electrostatic interactions between P_{11} peptides and LPS molecules, once the integrity of the LPS outer membrane was destroyed, the disruption of the cytoplasmic membrane could not be prevented. Additionally, the less adsorption of the P_{11} peptide to the lipids made it less wasteful during the bacterial killing processes. Because of such features, LPS may be considered as the receptor to some strongly cationic AMPs.

Sample	Layer	τ (Å)	Φ_{lipid}	$\Phi_{peptide}$	$\Phi_{solvent}$	A_{lipid} (Å^2)	Γ_{lipid} (10^{-6} mol/m^2)	$\Gamma_{peptide}$ (10^{-6} mol/m^2)
RcLPS (28mN/m)	Tail	13 ± 1	0.88 ± 0.11	0	0	198 ± 2	0.84 ± 0.08	0
	Head	23 ± 2	0.51 ± 0.05	0	0.49 ± 0.04	198 ± 2	0.84 ± 0.08	0
G_3 3μM +RcLPS	Tail	13 ± 1	0.75 ± 0.07	0.05 ± 0.01	0	N/A	0.70 ± 0.07	0.04 ± 0.01
	Head	23 ± 2	0.51 ± 0.05	0.05 ± 0.01	0.44 ± 0.04	N/A	0.83 ± 0.08	0.08 ± 0.01
G_3 30μM +RcLPS	Tail	13 ± 1	0.55 ± 0.06	0.35 ± 0.03	0	N/A	0.52 ± 0.05	0.33 ± 0.03
	Head	23 ± 2	0.32 ± 0.03	0.20 ± 0.02	0.48 ± 0.05	N/A	0.52 ± 0.05	0.33 ± 0.03
	Peptide	36 ± 4	0	0.10 ± 0.01	0.9 ± 0.1	N/A	0	0.26 ± 0.02
P_2 3μM +RcLPS	Tail	13 ± 1	0.48 ± 0.04	0.52 ± 0.05	0	N/A	0.44 ± 0.04	0.61 ± 0.06
	Head	23 ± 2	0.27 ± 0.02	0.05 ± 0.01	0.67 ± 0.06	N/A	0.44 ± 0.04	0.10 ± 0.01
P_2 30μM +RcLPS	Tail	13 ± 1	0.40 ± 0.04	0.6 ± 0.06	N/A	N/A	0.38 ± 0.04	0.7 ± 0.07
	Head	23 ± 2	0.23 ± 0.02	0.05 ± 0.01	0.70 ± 0.07	N/A	0.38 ± 0.04	0.1 ± 0.01
	Peptide	20 ± 2	0	0.10 ± 0.01	0.9 ± 0.1	N/A	N/A	0.18 ± 0.02
P_{11} 3μM +RcLPS	Tail	13 ± 1	0.63 ± 0.06	0.10 ± 0.01	0	N/A	0.60 ± 0.06	0.10 ± 0.01
	Head	23 ± 2	0.52 ± 0.05	0.26 ± 0.03	0.20 ± 0.02	N/A	0.88 ± 0.09	0.44 ± 0.04
P_{11} 30μM +RcLPS	Tail	15 ± 1	0.55 ± 0.05	0.2 ± 0.02	N/A	N/A	0.60 ± 0.06	0.22 ± 0.02
	Head	25 ± 2	0.50 ± 0.05	0.21 ± 0.02	0.29 ± 0.03	N/A	0.88 ± 0.09	0.39 ± 0.04
DPPG (28mN/m)	Tail	18 ± 2	1	N/A	N/A	48.0 ± 2	3.46 ± 0.40	N/A
	Head	10 ± 1	0.59 ± 0.06	N/A	0.41 ± 0.04	48.0 ± 2	3.46 ± 0.40	N/A
G_3 3μM +DPPG	Tail	20 ± 2	0.72 ± 0.07	0.12 ± 0.01	0.10 ± 0.05	N/A	2.77 ± 0.20	0.17 ± 0.02
	Head	24 ± 2	0.19 ± 0.03	0.23 ± 0.03	0.58 ± 0.06	N/A	2.77 ± 0.20	0.40 ± 0.04

G_3 30μM +DPPG	Tail	24 ± 2	0.64 ± 0.07	0.18 ± 0.02	0.15 ± 0.05	N/A	2.95 ± 0.30	0.31 ± 0.03
	Head	25 ± 2	0.20 ± 0.02	0.35 ± 0.06	0.45 ± 0.05	N/A	2.95 ± 0.30	0.64 ± 0.07
P_2 3μM +DPPG	Tail	19 ± 2	0.71 ± 0.08	0.19 ± 0.02	0	N/A	2.76 ± 0.30	0.32 ± 0.03
	Head	30 ± 3	0.25 ± 0.05	0.05 ± 0.02	0.70 ± 0.07	N/A	3.60 ± 0.40	0.04 ± 0.01
P_2 30μM +DPPG	Peptide	20 ± 2	0	0.5 ± 0.05	0.5 ± 0.05	N/A	0	0.90 ± 0.09
	Tail	25 ± 3	0.66 ± 0.07	0.22 ± 0.03	0.10 ± 0.05	N/A	3.19 ± 0.30	0.43 ± 0.05
	Head	32 ± 3	0.17 ± 0.02	0.25 ± 0.1	0.58 ± 0.10	N/A	3.19 ± 0.37	0.72 ± 0.30
P_{11} 3μM +DPPG	Tail	20 ± 2	0.88 ± 0.09	0.03 ± 0.01	0.08 ± 0.01	N/A	3.39 ± 0.30	0.04 ± 0.01
	Head	18 ± 2	0.32 ± 0.03	0.30 ± 0.10	0.38 ± 0.03	N/A	3.39 ± 0.30	0.40 ± 0.14
P_{11} 30μM +DPPG	Tail	20 ± 2	0.86 ± 0.09	0.05 ± 0.01	0.08 ± 0.01	N/A	3.28 ± 0.30	0.07 ± 0.01
	Head	18 ± 2	0.31 ± 0.03	0.40 ± 0.05	0.29 ± 0.04	N/A	3.28 ± 0.30	0.53 ± 0.06

Table 1: Parameters from the best model fits to the RcLPS and DPPG monolayers at the surface pressure of 28 mN/m. Peptide adsorption and lipid removal were determined after the equilibrated peptide binding following peptide injection.

Conclusion

Lipid monolayers as the mimicry of the cell membranes enabled us to characterise the structures upon APM binding. NR results demonstrated that cationic G_3, P_2, and P_{11} peptides had different extent of interactions to either DPPG or RcLPS monolayers. Peptide amphiphilicity dictates its antimicrobial activity. Peptides with stronger hydrophobicity (P_2) could penetrate further into the lipid tail region, but had the drawback of losing AMP molecules into bacterial membrane due to hydrophobic affinity. The electrostatic interaction of the positively charged AMPs and the negatively charged lipids endows peptide binding with the lipid head groups. But it is difficult for peptides with high cationicity and weak hydrophobicity (P_{11}) to disrupt even the full anionic DPPG monolayer. Strong anionic LPS molecules acted as the receptor to the P_{11} peptide and by accumulating a lot of peptide molecules on the membrane surface P_{11} finds an efficient route of killing *E. coli*.

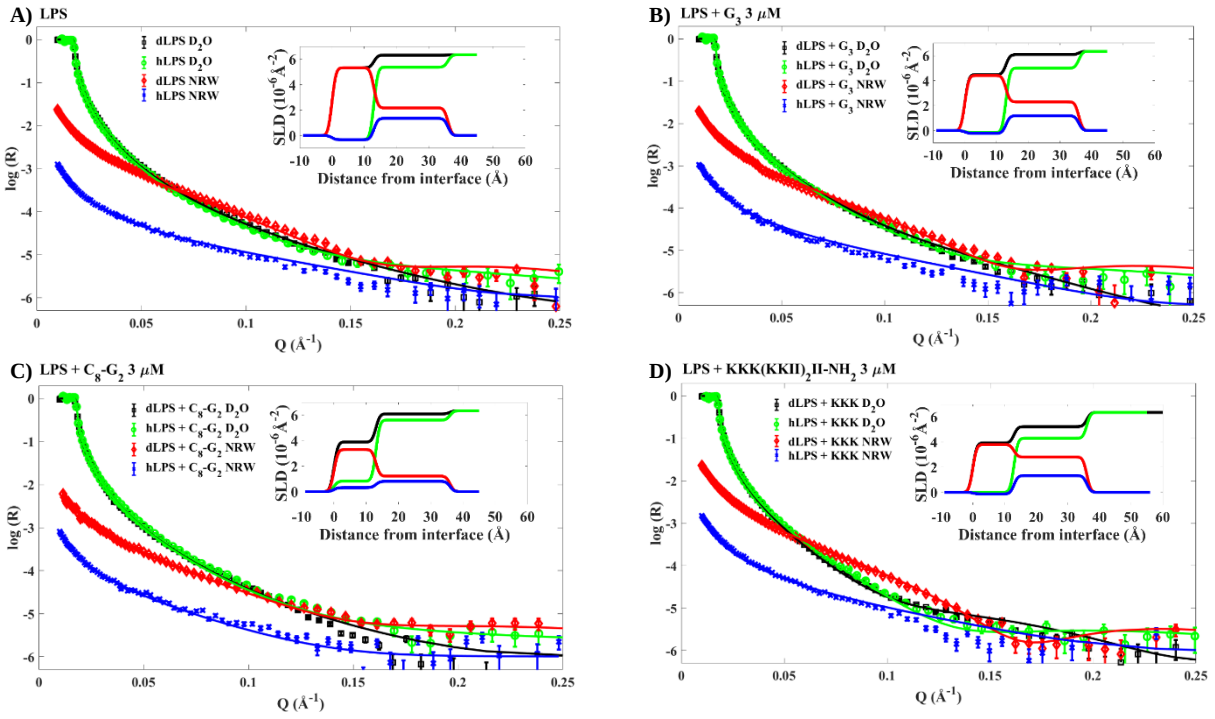

Figure 1: NR profiles and fits for (A) LPS monolayers at 28 mN/m and with the addition of (B) G_3, (C) P2, and (D) P11 peptides at 3 μM. The best fitted SLD profiles were presented in each plot.

References:

1. Hu, J.; Chen, C.; Zhang, S.; Zhao, X.; Xu, H.; Zhao, X.; Lu, J. R., Designed antimicrobial and antitumor peptides with high selectivity. *Biomacromolecules* **2011,** *12* (11), 3839-43.
2. Ciumac, D.; Campbell, R. A.; Clifton, L. A.; Xu, H.; Fragneto, G.; Lu, J. R., Influence of Acyl Chain Saturation on the Membrane-Binding Activity of a Short Antimicrobial Peptide. *ACS Omega* **2017,** *2* (11), 7482-7492.
3. Ciumac, D.; Campbell, R. A.; Xu, H.; Clifton, L. A.; Hughes, A. V.; Webster, J. R.; Lu, J. R., Implications of lipid monolayer charge characteristics on their selective interactions with a short antimicrobial peptide. *Colloids Surf B Biointerfaces* **2017,** *150*, 308-316.